

Supporting Information

$\text{Li}_3\text{V}_2(\text{PO}_4)_3$ particles embedded in N and S Co-doped porous carbon cathode for high-performance lithium storage: An experimental and DFT study

Jinggao Wu^{a,b,‡,*}, Canyu Zhong^{c,‡}, Xiaofan Chen^a and Jing Huang^{d,*}

^a Hunan Engineering Laboratory for Preparation Technology of Polyvinyl Alcohol Fiber Materials, Huaihua Key Laboratory for Preparation of Ceramic Materials and Devices, College of Chemistry and Materials Engineering, Huaihua University, Huaihua 418000, P. R. China

^b Chongqing Key Laboratory for Advanced Materials and Technologies of Clean Energies, School of Materials and Energies, Southwest University, Chongqing 400715, P.R. China

^c Panzihua Engineering Technology Research Center for Graphene, Panzihua University, Panzihua 617000, P.R. China

^d State Key Laboratory of Silkworm Genome Biology, Key Laboratory of Sericultural Biology and Genetic Breeding, Ministry of Agriculture and Rural Affairs, College of Biotechnology, P.R. China

* Corresponding authors.

E-mail addresses: jinggaowu@foxmail.com; hj41012@163.com.

‡ These authors equally contributed to this work.

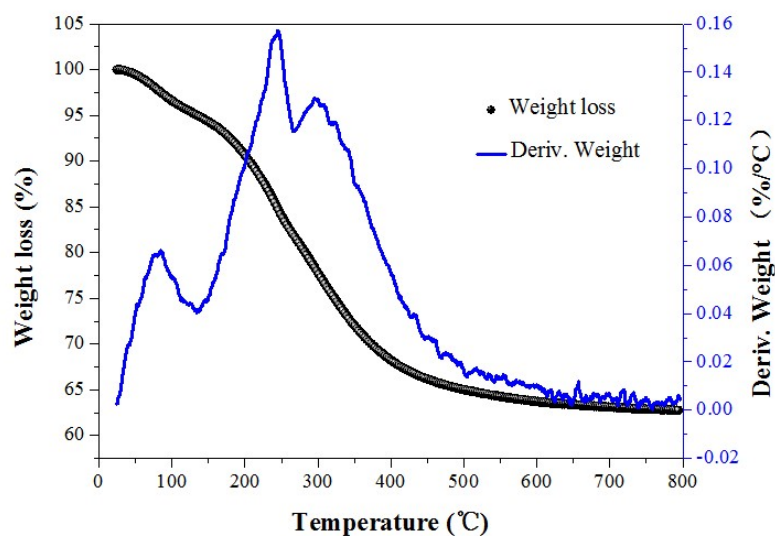


Fig. S1 TGA curve of LVP@C-NS12 was recorded under Ar atmosphere from 300 K to 1075 K.

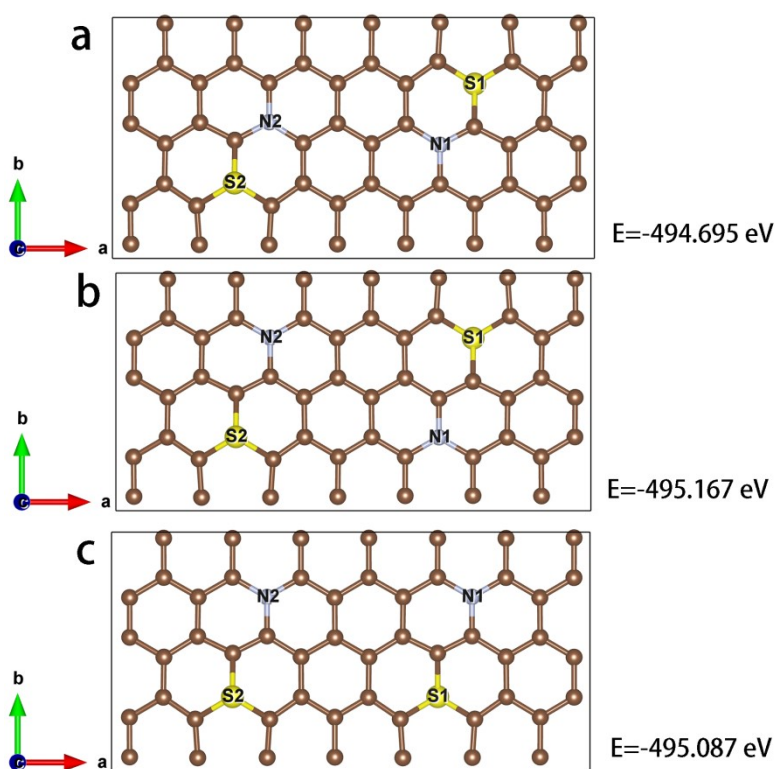


Fig. S2 Schematic illustration for the relaxed configurations of relaxed N,S co-doped C surface and its corresponding total energy: (a) coupled N and S, (b) isolated N and S type I, (c) isolated N and S type II co-doped carbon, respectively. The isolated N and S type I co-doped carbon shows the lowest total energy, which represents the most thermodynamically stable configuration.

The gray ball represents carbon.

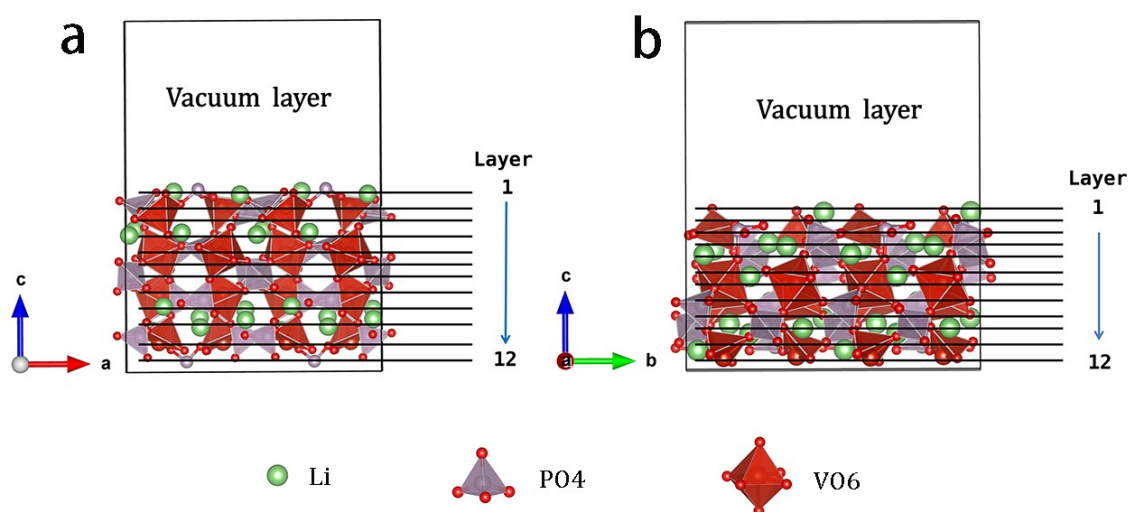


Fig. S3 Structural diagram of relaxed ($2\times 1\times 1$) clean surface: (a) LVP (001) surface; (b) LVP (010) surface.

Table S1 Calculated the surface energies(γ_s) results of the two surfaces of LVP at the PBE level.

Surface	$E_s^{unrelax}$ (eV)	$E_s^{unrelax}$ (eV)	γ_s (eV/Å ²)
$\text{Li}_3\text{V}_2(\text{PO}_4)_3$ (010)	-1037.38862	-1034.95809	0.158339
$\text{Li}_3\text{V}_2(\text{PO}_4)_3$ (001)	-1055.22511	-1059.12483	0.119695

The surface energy γ_s which describes the stability of a surface, is the energy required to cleave a surface from a bulk crystal. It can be calculated by the formula according to previous literature¹:

$$\gamma_s = \frac{1}{2A}(E_s^{unrelax} - NE_b) + \frac{1}{A}(E_s^{relax} - E_s^{unrelax})$$

Where, A is the area of the surface considered, $E_s^{unrelax}$ and E_s^{relax} is the energies of the unrelaxed and relaxed surfaces, respectively, N is the number of atoms in the slab and E_b is the bulk energy per atom.

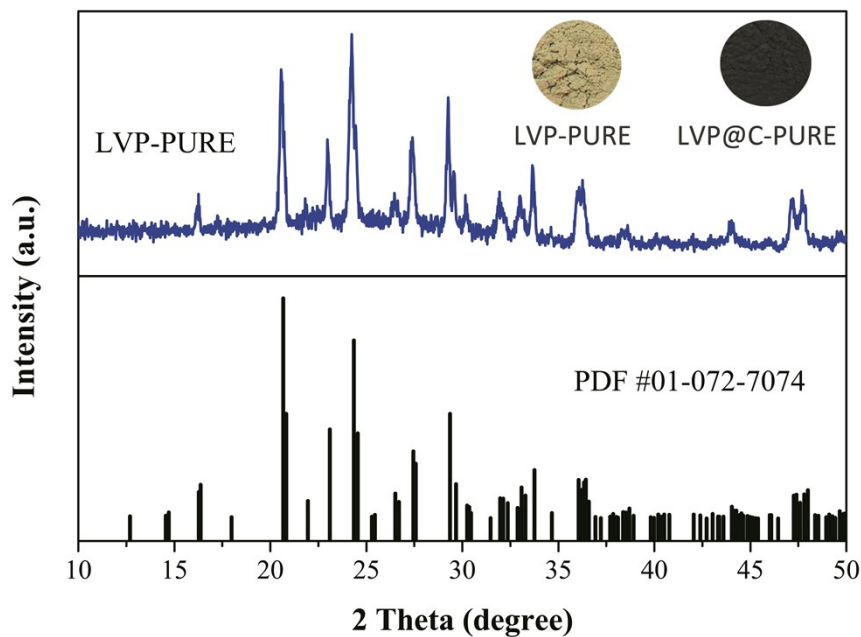


Fig. S4 XRD pattern of as prepared LVP@PURE sample.

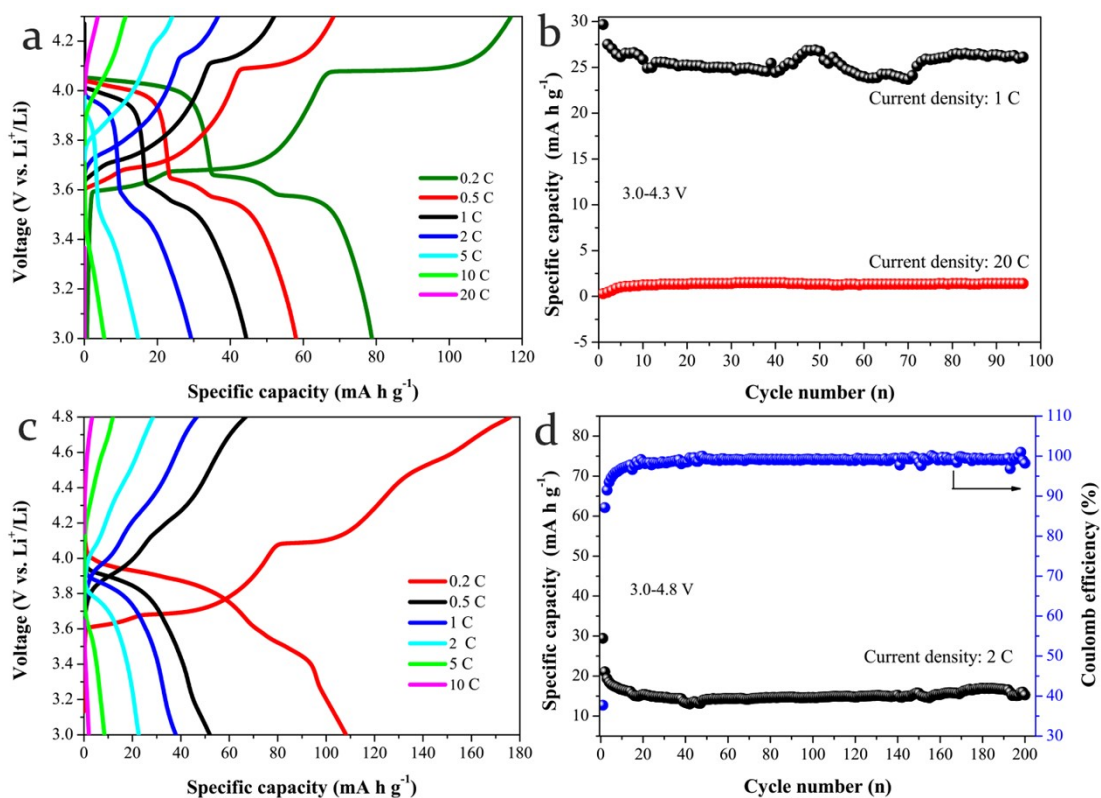


Fig. S5 GCD curves of LVP-PURE electrode at various current densities (a) and cyclic performance test at 2 C and 20 C rates (b) in a potential window of 3 - 4.3 V (vs. Li^+/Li , 1 C = 133 mAh g^{-1}); GCD curves of LVP-PURE electrode at various current densities (c) and cyclic performance test at 2 C rate (d) in the voltage range from 3 to 4.8 V (vs. Li^+/Li , 1 C = 197 mAh g^{-1}).

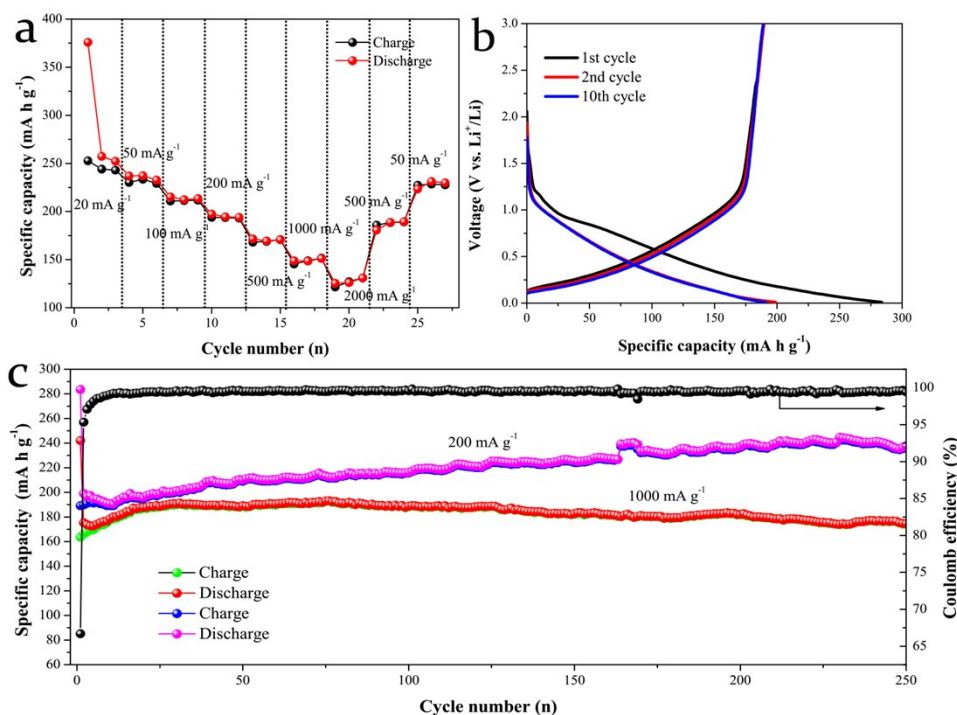


Fig. S6 (a).Rate performance of the commercial biomass hard carbon at different current densities. (b) GCD curves for 1st, 2nd and 10th at a current density of 200 mA g^{-1} . (c) Cyclic performance test at current densities of 200 and 1000 mA g^{-1} in a potential window of 0.01 - 3 V (vs. Li^+/Li).

Table S2 Comparison of specific capacities in this work to previous LVP@C-based cathode materials. (Note: NA-The value was not given in the paper.)

Samples	Initial capacities (mAhg^{-1})	Reversible capacities (mAhg^{-1})	Current density (mA g^{-1})	Cycles number (n)	Voltage window (V)	DFT calculations	References
LVP@C-NS12	123.82	117.42	133	100	3-4.3	Yes	This work
LVP@C-NS12	108.83	100.22	2660	500	3-4.3	Yes	This work
LVP@C-NS12	161.13	118.22	394	200	3-4.8	Yes	This work
LVP@ S doped C	146.1	116.0	197	100	3-4.8	No	[2]
LVP@N doped C	NA	79.8	1330	600	3-4.3	No	[3]
LVP@N doped G/C	97.1	101.3	2800	500	3-4.5	No	[4]
LVP- $\text{Na}_{0.04}$ @C	109.7	83.95	2660	1000	3-4.3	No	[5]
LVP@C/NCF	107.6	102.5	1330	1000	3-4.3	No	[6]
LVP@Dual Phase C	168.2	134	197	100	3-4.8	No	[7]
LVP-particle/fiber	121.09	119.55	133	500	3-4.3	No	[8]
LVP@C-fiber	149.92	107.69	197	500	3-4.8	No	[8]
LVP- $\text{Cu}_{0.05}$ @C	NA	105.4	2660	200	3-4.3	No	[9]
LVP@MWCNTs/C	112.9	91.67	1995	300	3-4.3	No	[10]
LVP- $\text{Pd}_{0.05}$ @C	111.9	93.78	665	150	3-4.3	No	[11]
LVP@C/3%CNT	98.7	96.1	1330	500	3-4.2	No	[12]
LVP/C-nf	94.11	72.72	133	500	3-4.3	No	[13]

References:

1. Q. Li, M. Rellán-Piñero, N. Almora-Barrios, M. Garcia-Ratés, I. N. Remediakis and N. López, Shape control in concave metal nanoparticles by etching, *Nanoscale*, 2017, **9**, 13089-13094.
2. C. Wang, Z. Guo, W. Shen, A. Zhang, Q. Xu, H. Liu and Y. Wang, Application of sulfur-doped carbon coating on the surface of $\text{Li}_3\text{V}_2(\text{PO}_4)_3$ composites to facilitate Li-ion storage as cathode materials, *Journal of Materials Chemistry A*, 2015, **3**, 6064-6072.
3. F. F. Guo, X. X. Zou, K. X. Wang, Y. P. Liu, F. Zhang, Y. Y. Wu and G. D. Li, $\text{Li}_3\text{V}_2(\text{PO}_4)_3$ particles embedded in porous N-doped carbon as high-rate and long-life cathode material for Li-ion batteries, *Rsc Advances*, 2015, **5**, 78209-78214.
4. M. Ren, M. Yang, W. Liu, M. Li, L. Su, X. Wu and Y. Wang, Co-modification of nitrogen-doped graphene and carbon on $\text{Li}_3\text{V}_2(\text{PO}_4)_3$ particles with excellent long-term and high-rate performance for lithium storage, *Journal of Power Sources*, 2016, **326**, 313-321.
5. Z.-L. Zuo, J.-Q. Deng, J. Pan, W.-B. Luo, Q.-R. Yao, Z.-M. Wang, H.-Y. Zhou and H.-K. Liu, High energy density of $\text{Li}_{3-x}\text{Na}_x\text{V}_2(\text{PO}_4)_3$ cathode material with high rate cycling performance for lithium-ion batteries, *Journal of Power Sources*, 2017, **357**, 117-125.
6. L.-L. Zhang, Z. Li, X.-L. Yang, X.-K. Ding, Y.-X. Zhou, H.-B. Sun, H.-C. Tao, L.-Y. Xiong and Y.-H. Huang, Binder-free $\text{Li}_3\text{V}_2(\text{PO}_4)_3/\text{C}$ membrane electrode supported on 3D nitrogen-doped carbon fibers for high-performance lithium-ion batteries, *Nano Energy*, 2017, **34**, 111-119.
7. X. K. Ding, L. L. Zhang, X. L. Yang, H. Fang, Y. X. Zhou, J. Q. Wang and D. Ma, Anthracite-Derived Dual-Phase Carbon-Coated $\text{Li}_3\text{V}_2(\text{PO}_4)_3$ as High-Performance Cathode Material for Lithium Ion Batteries, *ACS applied materials & interfaces*, 2017, **9**, 42788-42796.
8. J. Shin, J. Yang, C. Sergey, M. S. Song and Y. M. Kang, Carbon Nanofibers Heavy Laden with $\text{Li}_3\text{V}_2(\text{PO}_4)_3$ Particles Featuring Superb Kinetics for High-Power Lithium Ion Battery, *Advanced Science*, 2017, **4**, 1700128.
9. J. Yan, H. Fang, X. Jia and L. Wang, Copper incorporated in $\text{Li}_3\text{V}_2(\text{PO}_4)_3/\text{C}$ cathode materials and its effects on high-rate Li-ion batteries, *Journal Of Alloys And Compounds*, 2018, **730**, 103-109.
10. L.-B. Zhang, L.-Z. Wang and J. Yan, Synergistic growth of $\text{Li}_3\text{V}_2(\text{PO}_4)_3@\text{MWCNTs}@C$ nanocomposites as high-rate cathodes for Li-ion batteries, *Ionics*, 2018, **24**, 629-637.
11. Y. Zhang, High Rate Performance of Pd-doped $\text{Li}_3\text{V}_2(\text{PO}_4)_3/\text{C}$ Cathode Materials Synthesized via Controllable Sol-Gel Method, *International Journal of Electrochemical Science*, 2020, **15**, 6217-6226.
12. Y. Xia, L. Yu, C. Lu, J. Zhu, Z. Xiao, J. Zhang, C. Liang, H. Huang, Y. Gan and W. Zhang, Passion fruit-like structure endows $\text{Li}_3\text{V}_2(\text{PO}_4)_3@\text{C}/\text{CNT}$ composite with superior cyclic stability and rate performance, *Journal of Alloys and Compounds*, 2021, **859**, 157806.
13. Y. Lokeswararao, A. C. Dakshinamurthy, A. K. Budumuru and C. Sudakar, Influence of nano-fibrous and nano-particulate morphology on the rate capability of $\text{Li}_3\text{V}_2(\text{PO}_4)_3/\text{C}$ Li-ion battery cathode, *Materials Research Bulletin*, 2023, **166**, 112331.